Pharm Res (2015) 32:222–237
DOI 10.1007/s11095-014-1457-5

RESEARCH PAPER

Screening Methodologies for the Development of Spray-Dried Amorphous Solid Dispersions

Íris Duarte • José Luís Santos • João F. Pinto • Márcio Temtem

Received: 25 March 2014 / Accepted: 2 July 2014 / Published online: 19 August 2014

ABSTRACT

Purpose To present a new screening methodology intended to be used in the early development of spray-dried amorphous solid dispersions.

Methods A model that combines thermodynamic, kinetic and manufacturing considerations was implemented to obtain estimates of the miscibility and phase behavior of different itraconazole-based solid dispersions. Additionally, a small-scale solvent casting protocol was developed to enable a fast assessment on the amorphous stability of the different drug-polymer systems. Then, solid dispersions at predefined drug loads were produced in a lab-scale spray dryer for powder characterization and comparison of the results generated by the model and solvent cast samples.

Results The results obtained with the model enabled the ranking of the polymers from a miscibility standpoint. Such ranking was consistent with the experimental data obtained by solvent casting and spray drying. Moreover, the range of optimal drug load determined by the model was as well consistent with the experimental results.

Conclusions The screening methodology presented in this work showed that a set of amorphous formulation candidates can be assessed in a computer model, enabling not only the determination of the most suitable polymers, but also of the optimal drug load range to be tested in laboratory experiments. The set of formulation candidates can then be further fine-tuned with solvent casting experiments using a small amount of API, which will then provide the decision for the final candidate formulations to be assessed in spray drying experiments.

KEY WORDS Amorphous solid dispersion · miscibility · screening method · solvent casting · spray drying

ABBREVIATIONS

ASD(s)	Amorphous solid dispersion(s)
SDD(s)	Spray dried dispersion(s)
ITZ	Itraconazole
SC	Solvent casting
SD	Spray drying
HPMCAS-MG	Hydroxypropyl methylcellulose acetate succinate (grade MG)
PVP/VA 64	Polyvinylpyrrolidone-vinyl acetate copolymer
Eudragit® EPO	Copolymer of dimethylaminoethyl methacrylate, butyl methacrylate and methyl methacrylate
T_g	Glass transition temperature

INTRODUCTION

Currently more than 70% of the new chemical entities (NCEs) in the pharmaceutical pipeline present solubility constraints. According to the Biopharmaceutical Classification System (BCS), the percentage of these drugs (Classes II and IV) that actually reach the market is significantly lower - approximately 36% (1,2). In order to be aligned with the healthcare technological advances and to improve the bioavailability of these new drugs, it is imperative the consideration of physicochemical property enhancement technologies. Some examples of solubilization technologies are particle-size reduction, use of surfactants, salt formation, complexation with

Electronic supplementary material The online version of this article (doi:10.1007/s11095-014-1457-5) contains supplementary material, which is available to authorized users.

Í. Duarte • J. F. Pinto
iMed – Research Institute for Medicines and Pharmaceutical Sciences, University of Lisbon, Faculty of Pharmacy, Av. Prof. Gama Pinto 1649-003 Lisboa, Portugal

Í. Duarte • J. L. Santos • M. Temtem (✉)
R&D Drug Product Development, Hovione Farmaciência SA, Sete Casas 2674-506 Loures, Portugal
e-mail: mtemtem@hovione.com

cyclodextrines, production of self-emulsifying drug delivery systems and production of amorphous solid dispersions (3).

Over the last decade the production of stabilized amorphous drugs *via* amorphous solid dispersions (ASDs) has become an increasingly popular strategy to address the solubility challenge. The success of this formulation strategy is not only reflected in the significant number of marketed amorphous products (2,4), but also in the increasing percentage of ASDs demonstrating improved bioavailability when compared with the reference products (5). Nevertheless, there is still resistance among the pharmaceutical industry to adopt ASDs as a preferential strategy to improve drug solubility. One of the main reasons for such reluctance is related with the perceived risk of drug recrystallization followed by consequent loss of the solubility advantages created (6). The enhanced physical stability and protection against crystallization is related with the appropriate selection of formulation and process variables, which should be analyzed concurrently, from the early beginning of formulation development up to the commercial-scale manufacturing.

Among the variety of formulation variables that can affect the development of ASDs (*e.g.* drug and polymer physicochemical properties, selection of polymeric excipients, addition of surfactants, among others) the definition of the drug-polymer ratio is a critical parameter. Typically, scientists attempt to maximize the drug fraction in the formulation aiming the development of final oral-dosage forms (*i.e.* tablets or capsules) with reduced size (7,8). The optimal drug loading in the formulation should take into account drug potency, dose, solubility requirements, and most importantly, the maintenance of the physical state of the ASD. In this respect, the determination of the equilibrium crystalline drug solubility in the polymer and the drug-polymer amorphous miscibility has shown to be of great utility (9–12). Knowledge of these parameters and, particularly, on the thermodynamic phase diagram of the drug-polymer mixture helps to define the maximum drug to polymer ratio in the formulation minimizing the risk of recrystallization or phase-separation. Another important variable, still related to the latter, is the kinetic miscibility limit. In real terms, most ASDs are kinetically "trapped" in a non-equilibrium state, not only due to polymeric hindrance, but also to process and dynamic factors related to the typical energy-intensive methods of preparation considered (*e.g.* spray drying or hot-melt extrusion) (13). This is the reason why experimental drug loads are usually above the thermodynamic solubility and miscibility limit. Thus, it may be deem appropriate to define a "safe" kinetic miscibility design space, at early stages of drug product development, in which the formulator can operate without compromising the physical stability of the amorphous system.

A number of authors have been developing their own screening methodologies, either based on experimental data or based on theoretical fundamentals, to predict thermodynamic crystalline drug solubility (14–17) and drug-polymer amorphous miscibility. Regarding the latter, the analysis of the Hildebrand and Hansen Solubility Parameters (SPs) is one of the oldest methods (18–21). More recently, the implementation of lattice-based solution theories, such as the Flory-Huggins (F-H) model, were shown to be useful on the assessment of the thermodynamics of drug-polymer mixing. These methodologies have shown an acceptable predictability as a guide for polymer ranking, selection of initial drug-polymer ratios, manufacturing-ability and storage temperatures (11,12,22). However, these simple tools neither assess the influence of the preparation methods nor the process parameters (*e.g.* evaporation rate, mixing effect) on the level of drug disorder and distribution within the polymeric matrices (11). This may have an impact on drug load optimization and, consequently, one may not be taking full advantage of the amount of drug that the polymer can really "dissolve" or "incorporate". Thus, the current state-of-the-art would benefit from new theoretical models capable of describing both kinetic (typically process related factors) and thermodynamic considerations on the phase separation of a drug-polymer system.

The study presented proposes a new screening methodology intended to be used in the early development of ASDs. The novelty of this work consists on the implementation of a computational tool, based on diffuse interface theories, to guide rationale polymer selection and narrow the drug load range with potential to form homogenous amorphous systems. The most significant difference of this tool over other approaches (*e.g.* the use of the F-H theory alone) is the potential to evaluate a ternary system made of drug, polymer and solvent, by comparison with the traditional two-component system and the consideration of time-dependent phenomena, such as components mass diffusion and solvent evaporation. For assessing the effect of Thermodynamics, Kinetics and Evaporation (*i.e.* process variables) on the phase behavior of drug-polymer amorphous systems, this model (hereafter named TKE) was regarded as a pre-formulation tool in the development of amorphous dispersions using spray drying. To assess the applicability of this tool and have experimental evidence of the kinetic miscibility estimates, solid dispersions of a BCS Class II model drug – itraconazole (ITZ) - and structurally different polymers, known for having different compatibilities with ITZ, were produced using different solvent-based methods of solvent casting and spray drying.

MATERIALS AND METHODS

Materials

Crystalline ITZ was obtained from Chongqing Huapont Pharm.Co., Ltd (Chongqing, China). Three commercially

available polymers with different chemical and physical properties were selected: polyvinylpyrrolidone-vinyl acetate copolymer (PVP/VA 64, BASF, Ludwigshafen, Germany), dimethylaminoethyl methacrylate, butyl methacrylate, and methyl methacrylate co-polymer (Eudragit® EPO, Evonik Röhm GmbH, Darmstadt, Germany), and hydroxypropylmethylcellulose acetate succinate (HPMCAS grade MG, AQOAT®, Shin-Etsu Chemical Co., Ltd., Tokyo, Japan). The solvents used were methylene dichloride (DCM) and methanol (MeOH), both of analytical grade.

Methods

Fundamental Theoretical Considerations

This section summarizes the underlying theory and mathematical formalism of the model presented in this work. For more details on the derivation of the model readers are referred to the work of Saylor *et al.* (23,24)

TKE model is a system of partial differential equations (PDEs) based on diffuse interface theories (*i.e.*, Cahn-Hilliard and Allen-Cahn) to describe drug-polymer microstructure evolution. The physical basis of the model relies on fundamental thermodynamic, kinetic, evaporation equations to describe the influence of process conditions during microstructure formation.

Accounting for the thermodynamic contribution to microstructure evolution, the latter is related with the free energy density (*i.e.*, free energy per volume). The free energy (ΔG) is then modeled based on the F-H theory equation for a ternary system and is given by:

$$\frac{\Delta G}{nRT} = \phi_d \ln \phi_d + \phi_s \ln \phi_s + \frac{\phi_p}{m_p} \ln \phi_p + \chi_{ds} \phi_d \phi_s + \chi_{sp} \phi_s \phi_p + \chi_{dp} \phi_d \phi_p \quad (1)$$

where, n is total mole number, R is the ideal gas constant, T is the absolute temperature, Φ is the volume fraction of each of the components in the mixture (drug, polymer and solvent), m_p is the degree of polymerization and χ_{ij} is the F-H interaction parameter which accounts for the enthalpy of mixing.

Kinetic contributions are expressed by means of the diffusivities of the components, which are related with the implementation of the classic Fick's second law of diffusion:

$$\frac{\partial \phi_i}{\partial t} = \nabla \cdot D_{ij} \nabla \phi_j \quad (2)$$

where, t is the time and D_{ij} is the concentration-dependent diffusion coefficient of each of the components in the mixture. To comply with classical Fickian diffusion theory, two assumptions had to be considered, namely ideal mixing and interfaces were absent. The latter assumption implies that the systems are completely amorphous during microstructure formation.

To complete the derivation of this model, the following evaporation model was implemented:

$$\frac{\partial h}{\partial t} = k_e \phi_s \quad (3)$$

where, h is the height of the solution film, k_e is the evaporation rate coefficient and Φ_s is the volume fraction of the solvent. The evaporation of the solvent is homogenous across the liquid-vapor boundary and the solvent removal is described by a first-order rate coefficient.

Gathering all the equations together the system's microstructure evolution is governed by iteratively solving the PDEs, while aiming the minimization of the free energy of the system as a function of time. The simulations can be run in one or two-dimensions (1D or 2D, respectively) using a PDE solver software, such as FiPy version 3.1 (NIST, Gaithersburg, Maryland, USA) (25).

Implementation of the TKE Model

The application of the TKE model within the formulation field of new ASDs is anticipated to support the early identification of the theoretical kinetic miscibility region in which the amorphous system is homogenously mixed.

A schematic representation demonstrating a proposed flowchart for the application of the model, as a pre-formulation tool for the early development of ASDs is shown in Fig. 1. To run a simulation one must start with the definition of the input variables that are dependent upon the drug-polymer-solvent(s) system under study. These variables include thermodynamic and kinetic material-properties and process parameters. The material-properties are the F-H interaction parameters (χ_{ij}), the molar volume (V_m^i) and the diffusion coefficient of each component (D_i). To calculate these properties it is necessary to have information on the molecular structure of the formulation constituents. The process variables are the evaporation rate coefficient (k_e) of the spray drying process and the initial volume fraction of each component in the solution (Φ_i). All of these input parameters were calculated using the correlations described in the following sections.

Then, 1D simulations are run at the beginning of the process to screen the different systems and/or variables considered. In order to fine-tune the output or to improve clarity about phase-separation, 2D simulations should be considered. The latter are in general more time-consuming that the former. Whether in one or two dimensions, once the computational simulation starts, the solvent evaporates across the liquid surface and the drug-polymer microstructure begins

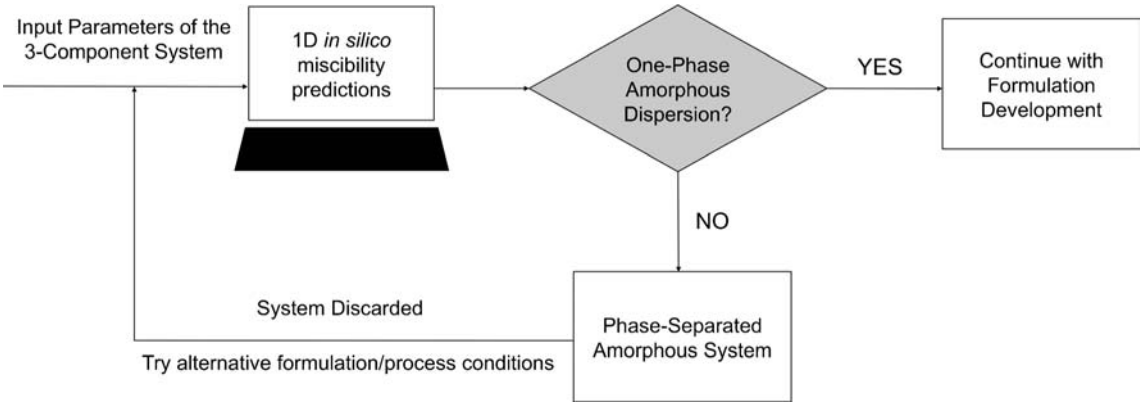

Fig. 1 Schematic representation showing the application of the TKE model as a screening tool for development of amorphous systems.

to evolve by diffusion, according to the molecular affinity between the ingredients. The final 1D microstructures are represented on a *x-y* plot, where the *y*-axis represents the final volume fraction of drug, polymer and solvent ($0<\Phi_i<1$) along the film's height, h_{film} (*x*-axis). On the contrary, the final 2D microstructures can be described as a matrix of volume fractions (drug, polymer or solvent) or composition map, where the *y-x* axes correspond to height and width (L_{film}) of the liquid film, respectively. In 1D simulations, homogeneity after solvent evaporation is characterized by relatively constant bulk volume fractions (drug and polymer) along the film height, while heterogeneity or phase-separation is indicated by abrupt shifts of the drug and polymer volume fraction curves along the *x*-axis. In case of 2D simulations, a homogenous system is represented as a composition map depicting a uniform color correspondent to a single final volume fraction, whereas different structures at sharp variations in colors correspond to the formation of different amorphous regions with different levels of drug concentration.

After conducting a computational simulation, if a homogenous amorphous mixture is obtained, such drug-polymer system can be considered a good starting point for further formulation development. Conversely, if the simulation indicates a phase-separated system with two distinct amorphous domains, the drug-polymer system may be considered physically unstable and alternative combinations (*e.g.* polymer, drug-polymer ratio, solvent composition) or changes of the process conditions should be considered (*e.g.* solution concentration, temperature).

Obtaining the Input Variables of the Model

F-H interaction Parameters

Three different F-H interaction parameters per system should be determined to apply the TKE model. These are the interaction parameters for the drug-polymer (χ_{dp}), drug-solvent (χ_{ds}) and polymer-solvent (χ_{ps}) pairs.

The interaction parameters can be calculated according to the following equation, using the Hildebrand solubility parameters:

$$\chi_{ij} = \frac{V_m^i}{RT}\left(\delta_i - \delta_j\right)^2 \tag{4}$$

where, V_m^i is the molar volume of the smaller component within the *ij* pair and δ is the Hildebrand solubility parameter.

In this work, χ_{ds} and χ_{ps} were calculated using Equation 4 with the data provided in Table I. When the solubility parameters are estimated using group contribution values, the respective interaction parameter obtained is an estimative at 298K (26). Due to this, it was decided to calculate χ_{dp} at the spray drying outlet temperature. This value will be more representative of the thermodynamic affinity during the formation of the microstructure.

To calculate an interaction parameter at non-ambient conditions, it is necessary to obtain the dependence of χ with temperature. According to the F-H theory and for polymer blends showing an upper critical solution temperature (UCST) behavior, it is accepted the following χ -T relation (10,27):

$$\chi_{ij} = A + \frac{B}{T} \tag{5}$$

where, *A* and *B* are fitting parameters that need to be determine in order to obtain χ_{ij} at any temperature.

Assuming that drug-polymer systems also exhibit an UCST, the temperature dependence of χ_{dp} can be described by Equation 5. The parameters *A* and *B* were determined by fitting a linear regression between two χ_{dp}'*s* obtained at two different temperatures. These temperatures were around the melting point of the drug (T_1), and at room temperature or 298K (T_2). To obtain χ (T_1) the melting point depression method was used for being a simple experimental method to obtain the interaction parameter at higher temperatures (9), while χ (T_2) was obtained using the Hildebrand solubility parameters (Table I). The experimental protocol for the

Table I Physicochemical properties of the raw materials considered in this work

Substance	MW [gmol^{-1}]	ρ [gcm^{-3}]	V_m [cm^{3}mol^{-1}] [a]	δ [(MPa)$^{1/2}$] [b]	T_g [°C] [c]
ITZ	706	1.27 [d]	556	24.77	59.2±0.3
HPMCAS-MG	18,000 [e]	1.29 [e]	13,846	23.49	120.3±0.7
PVP/VA 64	55,000 [e]	1.2 [e]	45,833	22.92	107.9±0.3
Eudragit® EPO	47,000 [e]	1.1 [f]	42,727	19.62	55.8±2.1
DCM	85	1.33	64	20.2	-
MeOH	32	0.79	40	29.7	-

MW: Molecular weight; ρ: True density; V_m: Molar volume; δ: Hildebrand solubility parameter; T_g: Glass transition temperature

[a] Calculated dividing the molecular weight by the true density

[b] Drug and Polymers: estimated at according to (37); Solvents: taken from reference (38)

[c] Obtained by mDSC – Mean ± s.d., $n=3$

[d] From reference (39)

[e] Supplier Information

[f] From reference (40)

melting point depression studies and associated results are presented as Supporting Information.

Diffusivity of the Components

The diffusivity of the solutes in the solvent was approximated to the diffusivity of the smaller component (i.e. drug) at 298K, since its molecular mobility is much higher when compared with the mobility of the polymer (28).

The drug's diffusivity was estimated using the Wilke-Chang equation (29):

$$D_{ds} = \frac{7.4 \times 10^{-8} \cdot T \cdot \sqrt{\alpha_s \cdot MW_s}}{\eta_s \cdot V_{m,d}^{0.6}} \quad (6)$$

where, D_{ds} is the diffusivity of the drug in the solvent, α_s is the association coefficient of the solvent and η_s the viscosity of the solvent.

Evaporation Rate Coefficient

The evaporation rate on the spray dryer was estimated according to the correlation for the drying of a single droplet in still air, according to Equation 7 (30):

$$\frac{dW}{dt} = \frac{k_d \, A \, MW_s}{RT}(P_{wb} - p_w) \quad (7)$$

where, k_d is the mass transfer coefficient, A is the droplet's surface area, T the drying temperature, P_{wb} is the vapor pressure of the solvent at the wet bulb temperature and p_w corresponds to the partial pressure of the solvent in the surrounding drying gas.

Equation 8 describes the mass transfer correlation for a spherical droplet in still air:

$$Sh = \frac{k_d \, d}{D_{sg}} = 2 \quad (8)$$

where, d is the droplet diameter, which was considered to be 30 µm (31), and D_{sg} is the diffusivity of the solvent vapor in the drying gas, which was estimated using the Fuller *et al.* correlation (32).

Regarding the estimation of P_{wb} and p_w, the former was calculated using Antoine's equation (32), and the latter was considered to be 10% of P_{wb}. The wet bulb temperature was estimated according to reference (33).

In the case of a solvent mixture, the evaporation rate was considered to be the evaporation rate of the solvent with the lowest vaporization enthalpy.

Volume Fraction

The initial volume fraction of each component in the solution can be calculated from the respective weight fraction (w_i) and the true density (ρ_i), based on Equation 9:

$$\phi_i = \frac{w_i/\rho_i}{w_i/\rho_i + w_j/\rho_j + w_z/\rho_z} \quad (9)$$

Solvent Casting (SC)

Cast films of ITZ and each polymer were obtained from solutions with 10, 15, 35, 45, 65 and 85% (w/w) ITZ. The total solids fraction was constant at 10% (w/w). The system ITZ:HPMCAS-MG was dissolved in a mixture of DCM:MeOH in a proportion of 80:20 (% w/w), whereas ITZ:PVP/VA and ITZ:Eudragit® EPO were dissolved in pure DCM.

A volume of approximately 40 μL of each stock solution was pipetted to a DSC aluminum pan to expedite direct analysis. At least three replicates of each drug-polymer system, at each drug fraction, were prepared. The sample holder was placed in a tray dryer oven at 40°C for 1 h, under vacuum to promote the rapid evaporation of the solvent. The goal was to design a SC experimental method as close as possible in terms of evaporation rate, to the subsequent spray drying process. The aluminum pans were sealed with the respective lids (pinholed) and directly placed in the sample tray of the calorimeter to be analyzed for the physical stability and experimental or kinetic drug-polymer miscibility capacity.

Spray Drying (SD)

Spray-dried prototypes of ITZ were produced at 45% and 65% (w/w) load with HPMCAS-MG, 45%, 65% and 85% (w/w) drug load with PVP/VA 64, and 15% and 35% (w/w) ITZ with Eudragit® EPO. Solutions of ITZ and each of the polymers were prepared with 10% w/w concentration of solids. The solvents used in the SD experiments were the same as those used in the SC tests.

Spray dried dispersions (SDDs) were produced in a laboratory scale spray dryer (BÜCHI Mini Spray Drier B-290, Switzerland). The spray drying unit was operated with nitrogen in single pass mode, *i.e.* without recirculation of the drying nitrogen. The drying gas fan was set at 100% of its capacity (flow rate at maximum capacity is approximately 40 kg/h). A flow rate of 0.76 kg/h was set for the atomization with nitrogen. The feed flow rate was set to 30% in the peristaltic pump (about 12 mL/min of liquid feed). The inlet temperature was adjusted to achieve an outlet temperature of 40°C. The SDDs were subjected to a post-drying step in a tray dryer oven with a temperature of 40°C for approximately 12 h, under vacuum.

At the end of the process, SDD powders were sampled and DSC pinholed aluminum pans were prepared. The products were analyzed for their physical stability and kinetic miscibility, according to the DSC analysis protocol described below. Powders were also analyzed by polarized light microscopy (PLM) to evaluate the presence of crystalline material.

Differential Scanning Calorimetry (DSC)

Conventional and modulated DSC (mDSC) experiments were performed in a TA Q1000 (TA Instruments, New Castle, Delaware, USA) equipped with a Refrigerated Cooling System (RCS). The enthalpy response was calibrated using indium. Three replicates of each sample, weighing between 5 and 10 mg were analyzed under continuous dry nitrogen purge (50 mL/min). Data was analyzed and processed using the TA Universal Analysis 2000 Software. The glass transition temperature was taken as the inflection point in the heat capacity change (ΔC_p) observed in the reversible heat flow, while exothermic and endothermic peaks were identified in the total heat flow.

Pure raw materials (ITZ and polymers) were analyzed using a modulated heating ramp from−10 to 250°C at a heating rate of 5°C/min using a period of 60s and amplitude of 0.8°C. It should be pointed out that crystalline ITZ had to be first subjected to a heat-cool-heat cycle (conventional DSC) to render the product amorphous, before applying the modulation cycle. Cast films and spray dried dispersions (SDDs) were analyzed using mDSC, but while for the latter the modulation conditions were the same as the ones used for the pure components, the amplitude used for the cast films was 1.6°C (*i.e.*, two times 0.8°C) in order to increase sensitivity.

DSC was applied to detect key indicators of homogeneity and phase separation of the cast films and SDDs. The number of amorphous phases present in the mixtures was defined based on the following generally accepted rules in the literature (11,34,35). If a single T_g value between the T_g's of the pure components is detected in the reversible heat flow, then one can consider that drug and polymer are homogenously mixed and a true amorphous solid solution (*i.e.* glass solution) was formed. Conversely, if two distinct T_g's corresponding to the pure components were detected, one can consider that amorphous-amorphous phase separation had occurred and an amorphous (or glass) suspension with polymer and drug rich phases was produced. For systems with higher drug loading is also common to detect other thermal events characteristic of phase-separation, namely recrystallization and melting during heating of the sample. Such events may correspond to the presence of crystalline material in the raw sample or may have been triggered by heating during the DSC run.

In this work, the detection of amorphous-amorphous phase separation can be facilitated by the fact that the molecule (ITZ) presents a mesophase (*i.e.* two endothermic peaks in the reversible heat flow around 69.6 ±1.0°C and 84.7±1.0°C) (36).

Polarized Light Microscopy

The SDDs powders were analyzed in a Nikon Labophot-2 Polarizing Microscope (Nikon, Japan) in order to detect crystalline material in the samples, by the presence of birefringence. Micrographs were taken using a TCA-9.0 Color Camera (Tucsen Imaging Technology Co. Ltd, China). Images were taken using the TSview 6.2.2.6 software.

RESULTS

F-H Interaction Parameter Calculation Using Solubility Parameters

The F-H interaction parameter (χ_{ij}) accounts for the enthalpic contribution for the Gibbs free energy of mixing (ΔG) and is a measure of the cohesive (intramolecular) and adhesive (intermolecular) interactions within the *ij* pair. Table I compiles important physicochemical properties of the solid compounds and solvents used in this work, to calculate the three F-H interactions parameters - drug-polymer (χ_{dp}), drug-solvent (χ_{ds}) and polymer-solvent (χ_{ps}) pairs.

Drug-Polymer Kinetic Miscibility Predictions

The phase behavior of the simulated systems will depend on the strength of the interaction between species and the process variables. The latter will dictate the formation of a homogenous and molecularly mixed ASD (*i.e.* amorphous solid solution), or on the other hand, an amorphous system showing phase separation of a drug- and polymer rich region (*i.e.* an amorphous suspension). The formation of two distinct amorphous regions is an indication of physical instability, and recrystallization may be observed when producing the respective dispersion (35). Thus, the model will only return one of two possible outcomes: homogeneity/heterogeneity, one-phase system/two-phase system or miscibility/immiscibility.

Figure 2 presents the sequence of 1D simulations for the drug-polymer systems in this study. A comparison of the kinetic miscibility predictions among the three pharmaceutical mixtures shows differences in drug-polymer phase behavior at the drying temperature.

In the case of the ITZ:HPMCAS-MG system, after solvent evaporation, both components remained homogenously mixed up to 85% (w/w) ITZ. The drug and polymer volume fraction curves in the 1D ITZ:HPMCAS-MG figures remained almost constant and parallel along the film height. No additional simulations were run for drug loads above 85% (w/w) ITZ.

In the case of the ITZ:PVP/VA 64 system, the drug and polymer remained homogenously mixed up to 45% (w/w) ITZ. For 35% (w/w) ITZ load the results suggest a potential for the system to separate into two phases, with the drug and polymer volume fraction curves showing an abrupt change in trend along the film height when compared to lower drug loads. With an ITZ concentration higher than 65% (w/w), the system was considered to be phase-separated, which was indicated by the formation of drug and polymer-rich amorphous regions along the film height.

Considering the results obtained, it can be said that the ITZ:PVP/VA 64 system was partial or locally miscible at the drying temperature and showed a miscibility discontinuity with increased drug loading. At this point, this miscibility discontinuity could be seen as a set of ITZ loads comprehended between 45% and 65% (w/w) drug fraction, which contained the maximum drug concentration from which the miscibility-immiscibility transition was observed.

Among the different drug-polymer systems studied, the pair ITZ:Eudragit®EPO presented the lowest drug-polymer kinetic miscibility, taking into account that the phase-separation was observed at the lowest drug load tested – 10% (w/w) ITZ. In this case, it can be postulated that a miscibility discontinuity exists for drug loads lower than 10% (w/w) ITZ. Drug loads lower than 10% (w/w) were considered to be below those used in practice, thus no further simulation was carried out for this system. By opposition, the reasons for not having run additional computational simulations for drug loads above 10% (w/w) ITZ:Eudragit® EPO were different. For drug-polymer systems presenting a miscibility behavior with a UCST (one of the assumptions considered in this work), above the critical temperature (T_c) drug and polymer form a homogenous system, while below T_c the drug-polymer system phase-separates. Analyzing the drug-polymer phase-diagrams reported in the literature by different authors, one can observe that they are highly asymmetric and shifted towards high drug loads (10–12,22,27). The critical compositions are generally above 80% (volume or weigh fraction) and the critical temperatures (T_c) are well above temperatures of interest with respect to spray drying processing (>100°C). These assume that for the drug-polymer systems under study and considering the temperature at which the kinetic miscibility predictions were run (T_{drying} =40°C), once the formation of a two-phase system occurred, heterogeneity was continuous up to 85% drug load (w/w), or another predefined upper bound by the user. The results from the 1D simulations of the ITZ:PVP/VA 64 corroborated the latter statement, showing drug-polymer phase separation above 65% ITZ (w/w).

Optimization of Drug Load – ITZ:PVP/VA 64 Case-study

In this section the drug load of the ITZ:PVP/VA 64 system was optimized within the miscibility transition range determined in the 1D simulations (45 to 65% w/w).

The first row in Fig. 3 shows the final 1D microstructures obtained after the evaporation of the solvent, while the second row corresponds to the final 2D microstructures with respect to the volume fraction of one of the components of the system, which in this specific case is the volume fraction of the drug (Φ_d). The 2D microstructures respecting the volume fraction of polymer and solvent (Φ_p and Φ_s, respectively) are not shown for sake of simplicity. The final polymer composition is the inverse of the drug, *i.e.* (1- Φ_d), while the solvent fraction is≈0 in the whole domain.

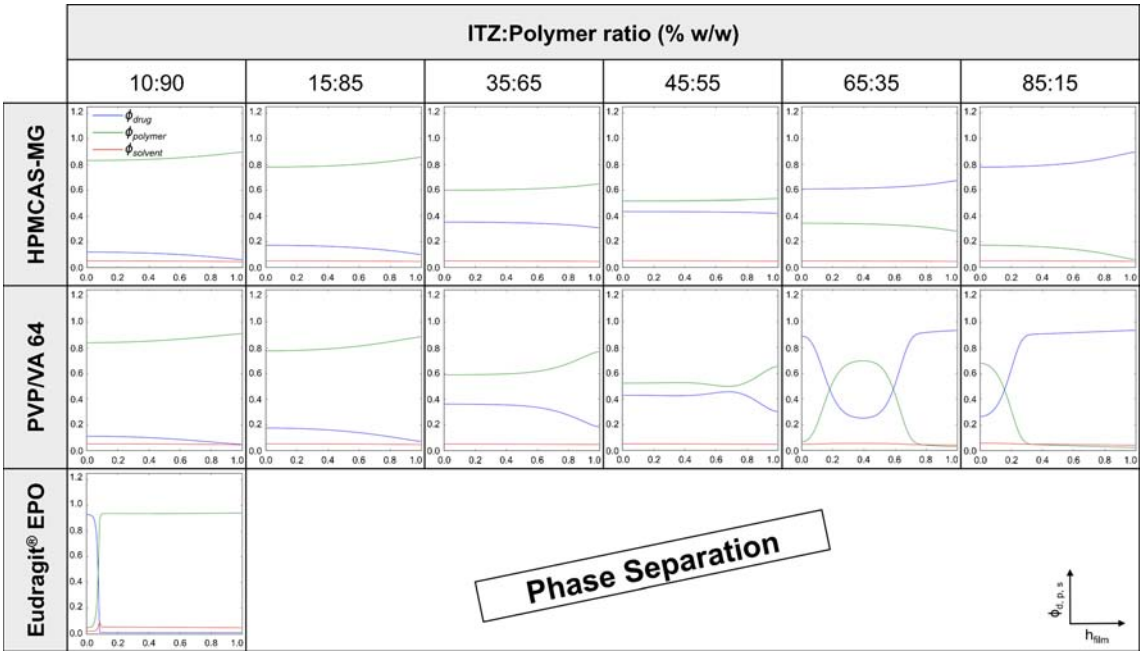

Fig. 2 Results from 1D simulations showing the theoretical final phase behavior of ITZ:HPMCAS-MG, ITZ:PVPVA/64 and ITZ:Eudragit® EPO with increasing drug concentration (*from left to right*). The 1D simulations show the final drug (*blue*), polymer (*green*) and solvent (*red*) volume fraction curves along the film height (*horizontal axis*).

Increments of 5% ITZ (w/w) were simulated in one- and two-dimensions starting with the 50% up to 60% ITZ:PVP/VA 64 (w/w) systems. The 1D and 2D figures obtained for 45% and 65% (w/w) loads were also included in Fig. 3 for comparison purposes.

The analysis of the 1D simulations in Fig. 3, indicates that phase-separation would occur above 50% (w/w) ITZ due to the formation of different layers or amorphous domains along the film thickness. However, the analysis of the respective 2D simulations has shown that, although apparent different amorphous regions have been formed in the 1D calculations, the 50% (w/w) ITZ system could be considered as a one-phase homogenous system in the 2D simulation, for presenting an overall constant volume fraction of drug around 0.4–

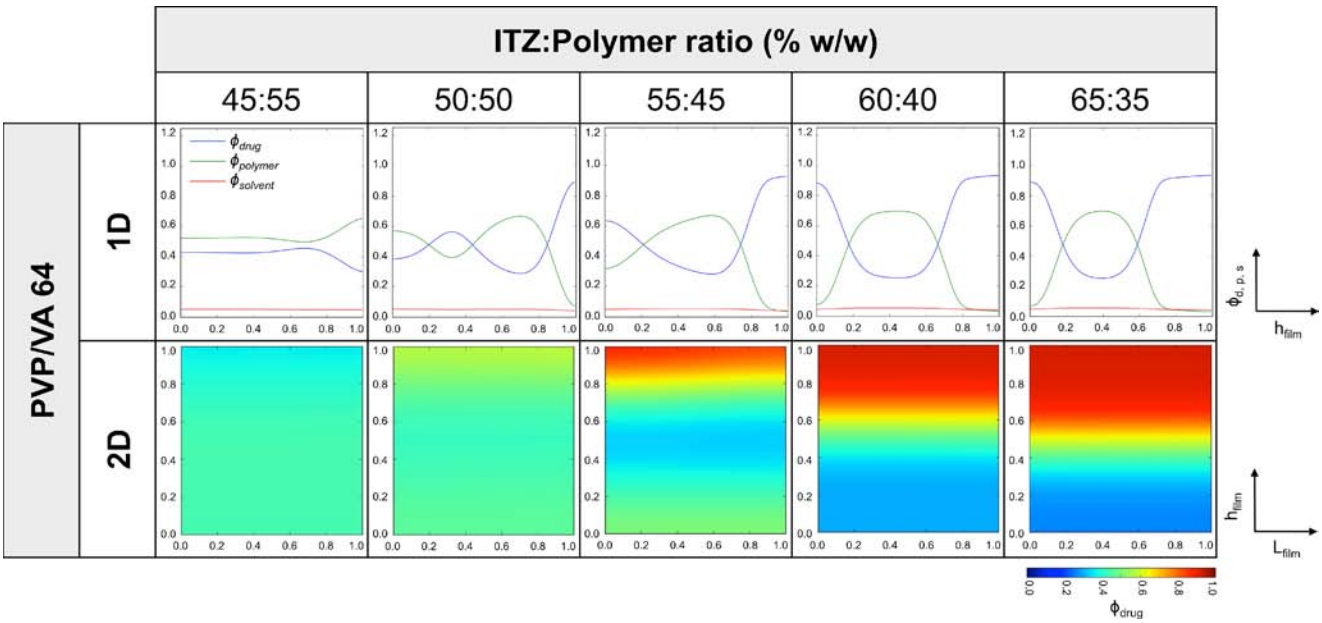

Fig. 3 Results from 1D and 2D simulations showing the phase composition of ITZ:PVPVA/64 system with increasing drug load within the kinetic miscibility discontinuity boundary (from 45 to 65% ITZ w/w).

0.5 along the film. This specific case illustrates well the importance and usefulness of 2D simulations if drug load optimization is desired.

At this point, the miscibility discontinuity or the drug load interval that contains the maximum theoretical drug load expected for the ITZ:PVP/VA 64 system was comprehended in the range between 50% and 55% (w/w) ITZ, and it could have been further narrowed down by executing an additional simulation at 52.5% (w/w) ITZ (Fig. 4).

Comparing the 1D simulations at 50% and 52.5% (w/w) ITZ, the final microstructures formed were fairly similar. According to the 2D simulations at 52.5 (w/w) ITZ, phase-separation with a clear segregation of two amorphous regions was more obvious, with one phase enriched in drug and the other in polymer. The drug load window from 50% to 52.5% (w/w) ITZ was now narrowed down so that one can infer that the theoretical maximum drug load the system can admit without compromising miscibility was ≈50% (w/w) ITZ.

Solvent Casting and Spray Drying Experiments

To assess the validity of the TKE model and to produce experimental evidence of the kinetic miscibility estimates, SC experiments were performed. The cast films produced were analyzed using mDSC to define the level of ITZ that could be added to the ASD before signs of phase-separation appear (either amorphous-amorphous or recrystallization). The drug load range between the maximum drug load added to the mixture before phase separation occurred, and the minimum drug load tested that exhibited signs of phase separation was defined as the SC miscibility discontinuity. Subsequently to the SC screening phase, SD prototypes were also produced. Drug-polymer spray drying experiments were undertaken according to the limits of the SC miscibility discontinuity. Only an additional ITZ:PVP/VA 64 SDD system was produced due to the detection of a false-negative result. This will be explained in more detail later in the text.

The DSC heat flow curves correspondent to the thermal analysis of the cast films and spray dried materials with drug loads equal to the SC miscibility discontinuity limits are presented in Fig. 5, Fig. 6 and Fig 7, for the systems ITZ:HPMCAS-MG, ITZ:PVP/VA 64 and ITZ:Eudragit® EPO, respectively. More detailed information (*i.e.* temperatures and micrographs) regarding the analytical characterization of the casted films and spray dried powders produced is presented as supporting information (Tables S2 to S3).

Figure 5 shows the mDSC profiles for the 45 and 65% (w/w) ITZ mixtures with HPMCAS-MG prepared by solvent casting and subsequent spray drying. In what regards the cast films, at 45% (w/w) ITZ the product presented a single glass transition temperature (T_g) in the reversible heat flow (shown by an arrow) and a single relaxation endotherm in the non-reversible heat flow (not shown). No signs of amorphous-amorphous phase separation or crystallization were observed in the thermograms. Profiles for the 10, 15 and 35% (w/w) ITZ loading cast films were identical to the 45% (w/w) ITZ (Table S2, Supporting Information).

The results suggest that ITZ was homogenously mixed and molecularly dispersed within HPMCAS-MG up to 45% (w/w) drug load. In the case of 65% (w/w) ITZ:HPMCAS-MG cast films, the only change in heat capacity detected in the reversible heat flow profile was around 26.7±4.2°C, a temperature significantly below from the one expected, considering the T_g of the pure components or even considering the mixed T_g value decay due to increasing ITZ loading, according to the Gordon-Taylor equation (41). No phase-separation or recrystallization events were detected during heating, but an endothermic peak at 151.6±1.2°C was observed. This endothermic peak might correspond to the melting of ITZ (T_m=162.6±0.2°C). The

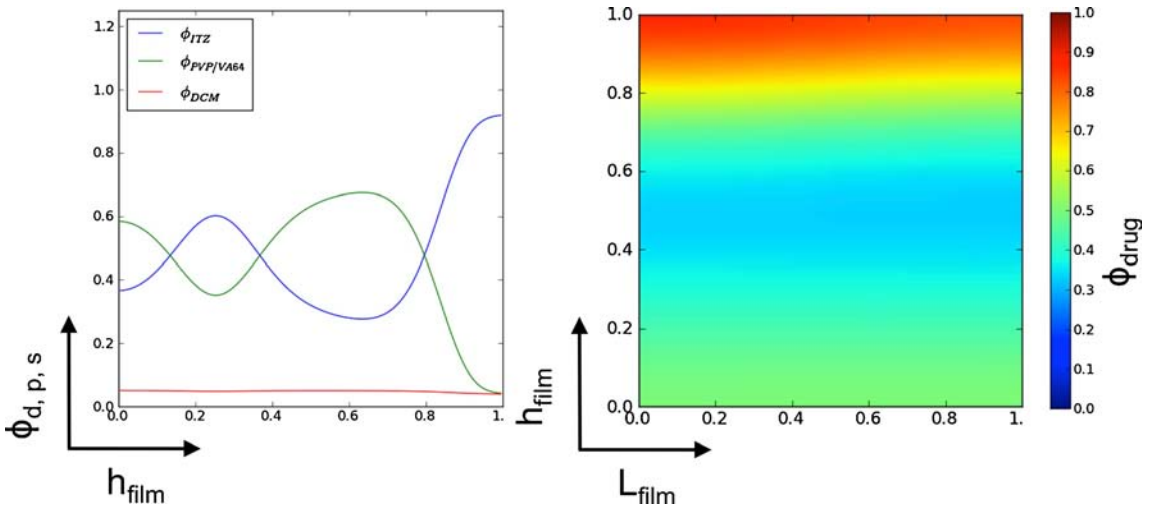

Fig. 4 Results from 1D and 2D simulations showing the final phase behavior of ITZ:PVPVA/64 system at 52.5% (w/w) ITZ.

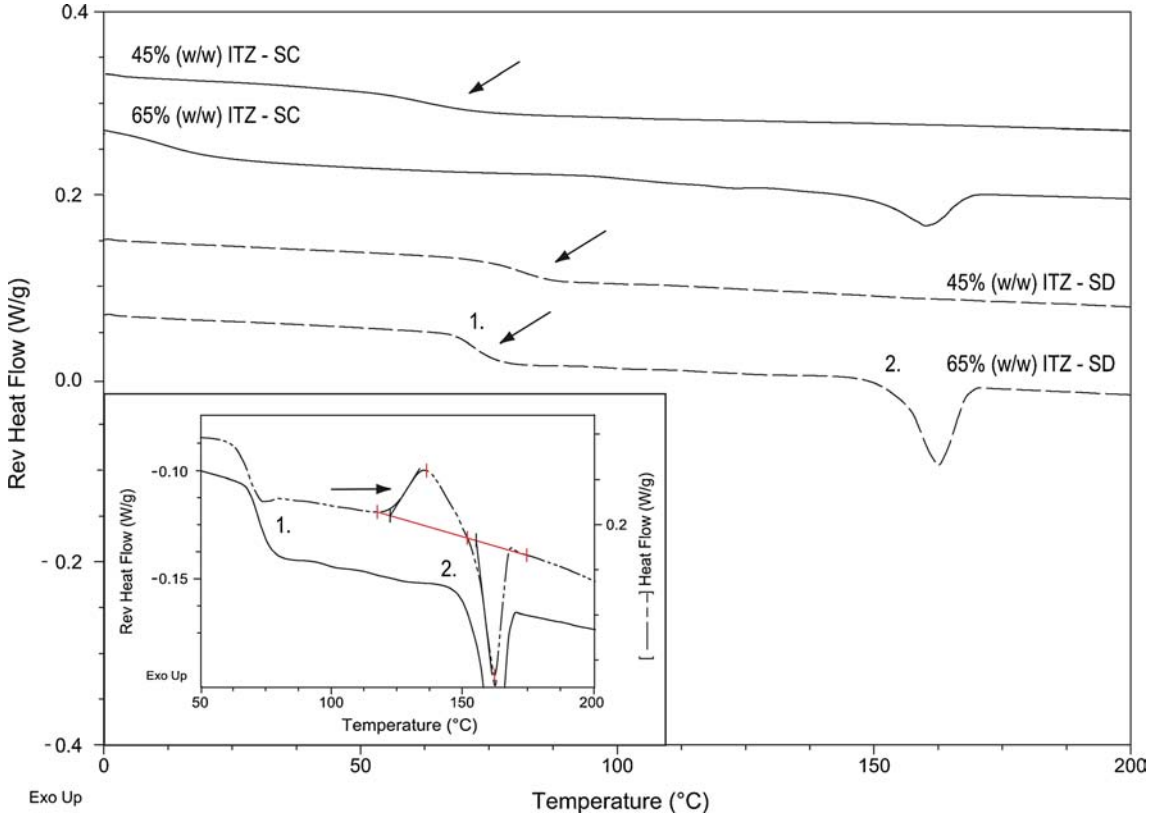

Fig. 5 Reversible heat flow thermograms for the 45 and 65% (w/w) ITZ:HPMCAS-MG cast films (*solid line*) and respective spray-dried materials (dotted line). Arrows indicate the T_g's.

melting point depression observed was due to the presence of the polymer that lowered the chemical potential of the drug and led to a decrease of its melting temperature (13,42).

The existence of an endothermic event without the observation of a prior exothermic recrystallization also presupposes the presence of a starting crystalline material in the sample. This observation could be related to the absence of a mixed T_g, thus with the formation of heterogeneities along the cast film due to *e.g.* poor drying conditions, inefficient process of amorphization or residual solvent plasticizing the product. The 85% (w/w) ITZ:HPMCAS-MG casted films showed a single T_g value near the T_g of pure ITZ, but considering that neither the drug mesophase nor the T_g of the polymer were detected, a homogenous amorphous system might have been formed. However, the system evolved into recrystallization followed by melting of the drug, during the heating cycle (Table S2). Recrystallization triggered by heating is a consequence of increased molecular mobility and molecular rearrangement in amorphous systems with high drug load and insufficient polymeric stabilization (43). Such systems are considered less stable and are more prone to phase-separation and drug crystallization triggered by external variables (*e.g.* temperature, humidity) (20,44).

Both the thermograms of the 45% (w/w) ITZ cast film and the SDD presented a single T_g in the reversible heat flow without signs of amorphous-amorphous phase separation or recrystallization, suggesting the formation of an amorphous solid solution. Moreover, no birefringence was observed in the sample. The thermogram of 65% (w/w) ITZ SDD has shown that the heterogeneities formed during SC disappeared and gave place to a clear mixed T_g with the respective relaxation endotherm in the non-reversible heat flow (not shown). The absence of birefringence by microscopy also indicated the formation of a homogenous ASD. However, this system like the one with 85% (w/w) ITZ cast film was not stable on heating; the drug recrystallized prior to melting (Fig. 5, insert). Although SD promoted a more efficient amorphization process with a faster entrapment of the components of the solution, the high drug load in formulation may present a higher risk of structure destabilization and physical instability.

Figure 6 presents the mDSC thermograms for the ITZ:PVP/VA 64 binary mixtures manufactured by the solvent casting and spray drying processes. For casted films with 45% (w/w) ITZ no recrystallization or melting endotherms were detected and only a single mixed T_g was observed. On the other hand, for lower drug loads (10, 15 and 35% (w/w) drug load) no conclusion regarding the physical-state of these systems can be drawn by the analysis of the thermograms. In the three replicates, unexpected endothermic events appeared at 80°C and 150°C in the total heat flow. Janssens *et al.* also

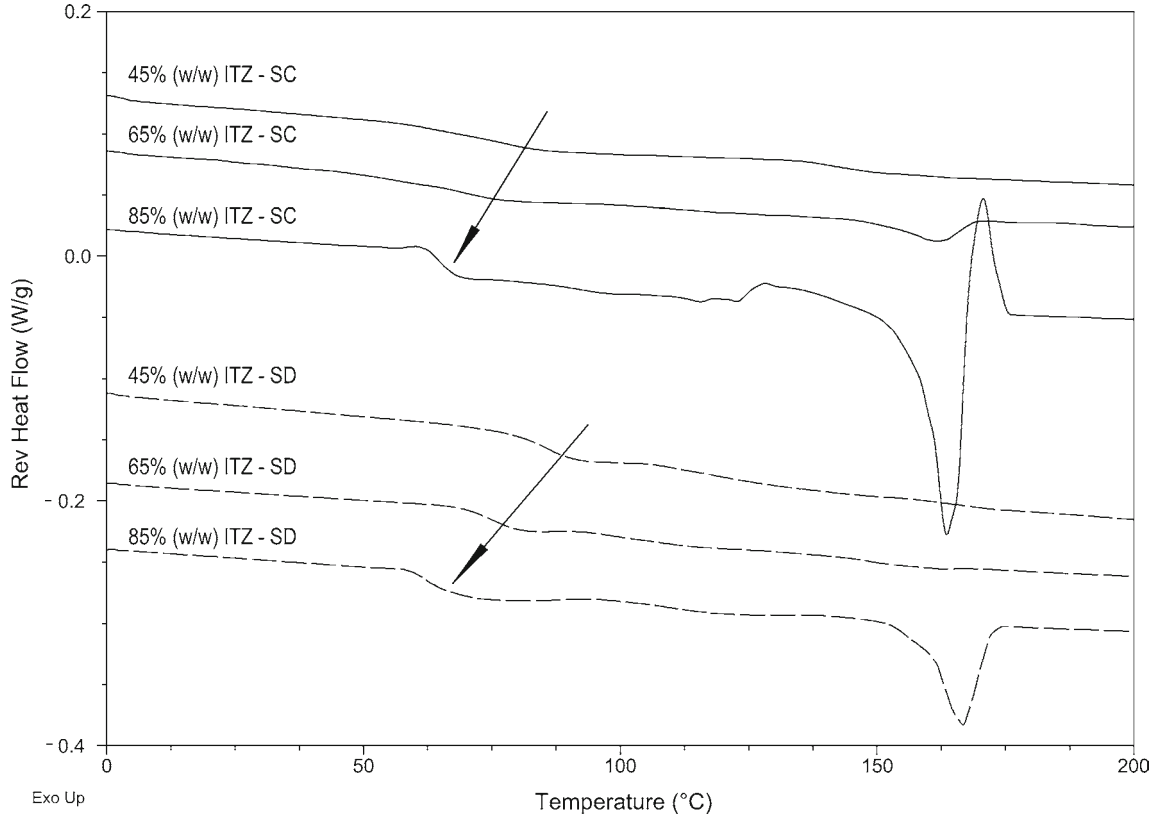

Fig. 6 Reversible heat flow thermograms obtained for the 45, 65 and 85% (w/w) ITZ:PVP/VA 64 cast films (*solid line*) and respective spray-dried materials (dotted line). Arrows indicate the T_g's.

observed endothermic events in the range of 40°C and 100°C in the mDSC thermograms of ternary systems made up of 10, 20 and 40% (w/w) ITZ load in 25/75 (w/w) TPGS 1000/PVPVA 64 (45). These authors justified the appearance of such events as relaxation enthalpy peaks correspondent to the formation of amorphous inhomogeneities in the samples. To validate this hypothesis, they performed a heat-cool-heat cycle with those materials in the calorimeter, and the endothermic peaks disappeared in the second heating run. This second heating eliminated the thermal history of the samples and potential amorphous phases present in the raw material disappeared (34).

In this work, amorphous inhomogeneities may have also been formed in the cast films. Although additional tests could have been performed, the indication of the production of an amorphous and homogenous system containing a higher drug load [*i.e.* 45% (w/w)] was sufficient to move forward with the screening method.

Increasing the ITZ potency to 65% and 85% (w/w), the cast films presented a single T_g and considering the absence of a drug mesophase or second T_g in both systems, this was a strong indication that the drug was homogenously mixed with the polymer. Still, upon increasing the drug loading to 65% (w/w), a slight melting endotherm was detected, while increasing the ITZ potency to 85% (w/w) caused a large melting endotherm. Both compositions have shown a recrystallization exotherm when analyzing the total heat flows.

The SD results from the respective SDDs with 45% and 65% (w/w) ITZ exerted a single mixed T_g and no signs of amorphous-amorphous phase separation or crystallization, which suggests that amorphous solid solutions were formed. Consequently, one can refer that the cast film with 65% (w/w) ITZ was a false-negative result. This observation reinforces the fact that although solvent casting can provide useful preliminary information on kinetic miscibility and physical stability, premature conclusions should not be drawn from the analytical results of the cast films; again, one may be neglecting the real solubilization capacity offered by the polymer. This shows the importance of confirming the SC results with the production of the respective SDDs.

In order to determine the experimental kinetic miscibility limit of the ITZ:PVP/VA 64 mixture, an additional SD experiment at 85% (w/w) ITZ was performed. Upon increasing the ITZ loading, despite the detection of a mixed T_g, a recrystallization peak followed by melting was observed. No glassy ITZ clusters were detected, but according to the PLM results, ITZ crystallites were present. The results obtained indicate that at 85% (w/w) ITZ, even using such drying process

conditions, the drug cannot be completely stabilized by the polymer. Comparing with 85% (w/w) ITZ:PVP/VA 64 cast film, the thermal results were similar (Table S2-S3).

Finally, Fig. 7 shows the thermal results for the 15% and 35% ITZ:Eudragit® EPO cast films and respective spray dried powders. Amorphous solid solutions without the detection of key indicators of physical instability were produced via SC, up to and including 15% (w/w) drug load. Contrarily, when increasing the ITZ load to 35% two single T_g's and the ITZ mesophase were detected in the reversible heat flow. The zoom in Fig. 7 shows the relaxation endotherms correspondent to the phase-separation event. The 45% cast films also present signs of amorphous segregation within the same temperature range. It is difficult to conclude with certainty if these two T_g's correspond to the complete segregation of two phases or to the formation of amorphous clusters of ITZ, still with a certain percentage of drug molecularly dispersed within the polymer (glass suspension/solution) (46,47). It was also noted that, while the 35% (w/w) ITZ cast films remained kinetically stable as phase-separated systems and any additional events were detected during heating, the 45% system presented drug recrystallization and melting. For the 65% and 85% (w/w) cast films, the formation of drug amorphous clusters was observed (detection of mesophase), however only one T_g was detected. For those cases, the detection of two single T_g's may be hidden by the detection of a broad T_g value.

The results obtained for the spray-dried materials produced were consistent with the respective SC profiles. At 15% (w/w) ITZ load a single-phased amorphous system was obtained with no observation of further events during heating, while at 35%, though the SDD presented one single T_g it has evolved into crystallization of the drug during the heating cycle.

DISCUSSION

Over the last few years, there was a growing interest by the pharmaceutical industry, in the implementation of screening methodologies to support the development of ASDs. The basis for this change might be related to the application of Quality by Design (QbD) principles and concepts, where one of the main goals is to *build quality into the product*, thereby reducing empiricism, development time, risk and costs (48).

Screening methodologies should include, but not be limited to, the assessment of the thermodynamic drug solubility in the polymer and drug-polymer kinetic amorphous miscibility. Effective screening tools should provide the answer to key

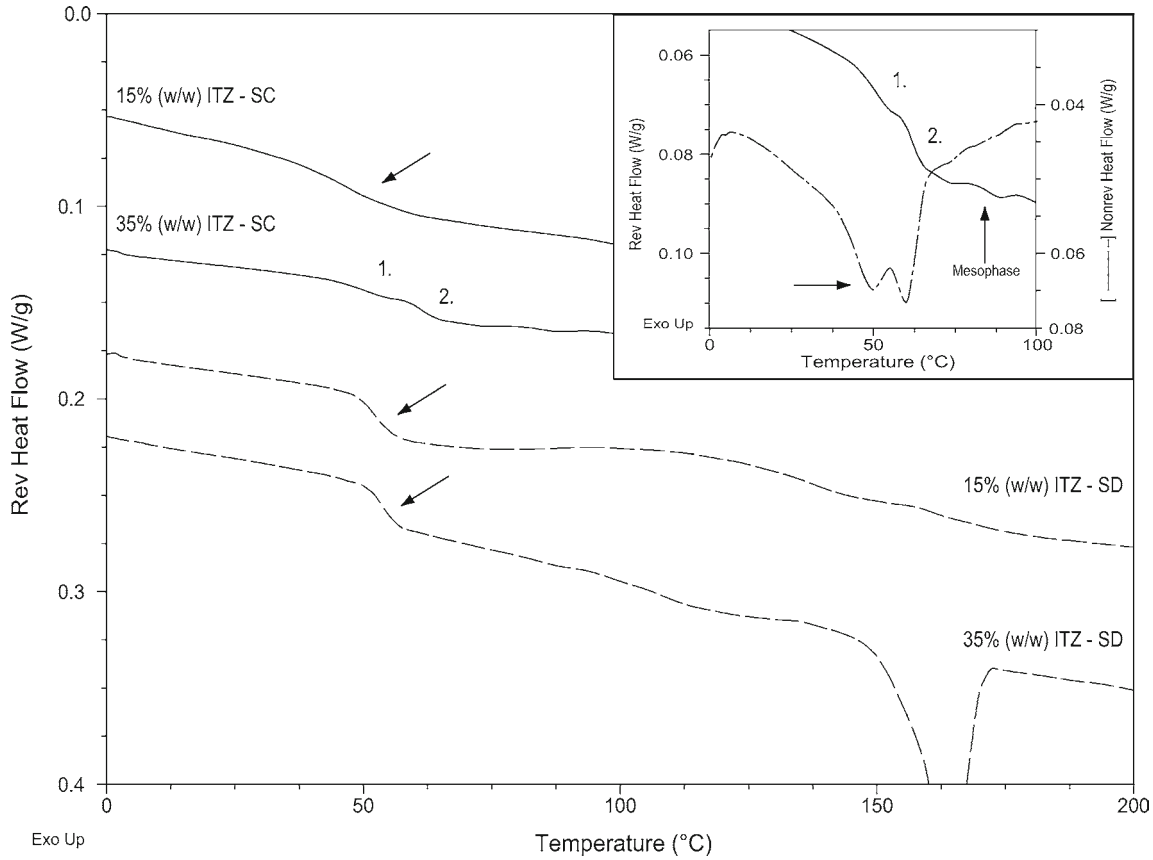

Fig. 7 Reversible heat flow thermograms obtained for the 15 and 35 (% w/w) ITZ:Eudragit® EPO cast films (*solid line*) and respective spray-dried materials (*dotted line*). Arrows indicate the T_g's.

questions, such as, what are the most suitable polymers and process variables that allow the manufacturing of high-dose formulations showing improved physical stability during product development and long-term storage.

The study presented proposes a new screening methodology intended to be used in the early development of ASD produced by spray drying. The novelty of this work is the implementation of a computational tool to guide rationale polymer selection and the narrowing of drug load ranges with the potential to form miscible binary systems. The major differences of the TKE model implemented from commonly applied methodologies to predict the solubility and miscibility of a drug in a polymeric carrier are the assessment of the thermodynamics of mixing of a drug-polymer-solvent system, the inclusion of kinetic material properties and process variables (*i.e.*, components diffusion and evaporation rate, respectively). The use of this model allows the definition of the kinetic drug-polymer system phase boundaries, as it will also provide detailed information regarding the influence of important process variables (e.g. selection of the solvent, concentration of solids in the solvent, drying temperature) on the limits of this miscibility region.

As a first assessment of the validity of the TKE model, three amorphous pharmaceutical systems composed of ITZ and PVP/VA-64, HPMCAS-MG and Eudragit® EPO were tested. 1D computational simulations were run, and in order to have an experimental evidence of the kinetic miscibility estimates a SC experimental protocol was developed. Cast films were produced with the same drug-polymer systems, at the same drug loads and process conditions (*i.e.* drying temperature) as the computational simulations tested. Then, the scale-up of the systems correspondent to the limits of the SC miscibility discontinuity using spray drying further confirmed the validity of the model and the screening methodology as a whole.

In order to analyze the results obtained together, Fig. 8 compiles in a single schematic representation the theoretical predictions provided by the TKE model and the analytical results obtained for the casted films and spray dried products for the different ITZ amorphous systems studied.

The results are depicted by means of continuous bars, which represent the kinetic miscibility behavior as a function of drug loading for each ITZ system studied. According to the results that have already been described in previous sections, grey bars were extended up to the maximum drug load tested that each polymer could stabilize without the existence of signs of physical instability. By opposition, black bars were extended from the minimum drug load tested with the detection of two amorphous regions (A-A) or the presence of crystalline material suspended in the amorphous matrix (C-A). The presence of crystalline drug in the product may have origin from incomplete amorphization, or recrystallization during the DSC heating run. The uncertain region bars correspond to what was defined as the miscibility discontinuity or the region that includes the drug loading from which phase separation is observed or inferred from the results.

It should be noted that the representation of the bars are supported on discrete experimental points, bearing in mind that a lower number of tests were performed for the representation of the spray drying bars. It is assumed that these miscibility interpolations can be considered and that these are valid within the assumption that drug-polymer pharmaceutical systems in general present a typical temperature-composition phase diagram, *i.e.* the asymmetrical "inverted U" presenting only an UCST, shifted for higher drug loads (10–12,22,27).

Validation of the TKE Model and Screening Methodology

Analyzing Fig. 8 and comparing the miscibility estimates and the experimental results of the casted films and spray-dried products of each drug-polymer system, it can be seen that the TKE is able to globally describe the amorphous drug-polymer compatibility and phase behavior. For example, the drug-polymer pairs which exhibited a higher experimental miscibility capacity, *i.e.* around 45% (w/w) for the ITZ:HPMCAS-MG and 65% (w/w) for the ITZ:PVP/VA 64 system, were those which simulations indicated the formation of a homogenous amorphous systems for higher drug loads [85% and 50% (w/w) ITZ, respectively]. In a similar way, the drug-polymer mixture which presented its maximum of experimental miscibility at lower drug loads, *i.e.* around 15% (w/w) for the ITZ:Eudragit® EPO system, was the one where the model predicted phase-separation for lower drug loads [10% (w/w) ITZ].

These results suggest that the TKE model can be used successfully to rank the best polymers for amorphous drug stabilization. In this study, the following ranking would be obtained by ascending order of kinetic miscibility capacity for the ITZ systems tested: Eudragit® EPO << PVP/VA 64 < HPMCAS-MG.

As far as the maximum miscibility values obtained are concerned, some differences were identified for the predicted and observed results. Despite including the influence of thermodynamic, kinetic and dynamic factors on the final phase behavior of ASDs, TKE may not fully capture the complexity of drug-polymer particle formation. The causes that contribute for these differences may be seen from a three level perspective, *i.e.* starting from the global design and structure of the computational tool taking into account the objectives for which the model was originally developed, considering simultaneously the limitations and assumptions of the models applied, especially in what regards the F-H theory and the evaporation model, and finally the simple experimental methods and correlations used to estimate part of the

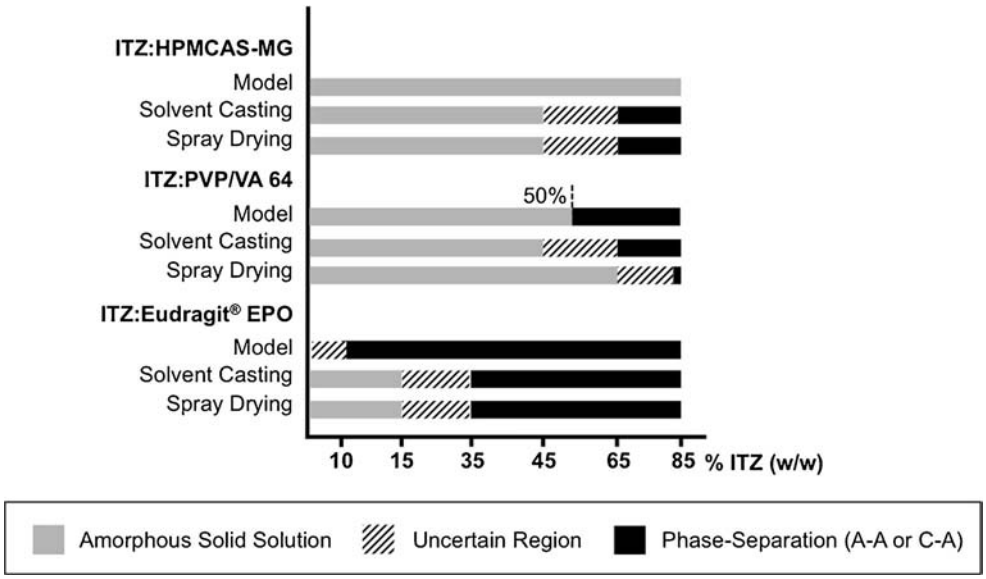

Fig. 8 Theoretical miscibility predictions given by the TKE model and analytical results obtained for the solvent casting films and spray drying products, as a function of drug load.

system-dependent input parameters. Thus, the accuracy of the predictions should be analyzed in light of the limitations and assumptions of the computational system.

Although validation from a quantitative standpoint should not be made at this point of the work, it is still possible to use the kinetic miscibility estimates obtained from the model to create some guidelines to define a narrow drug load range to be tested using solvent casting or spray drying. Moreover, we can use all the information gathered (TKE+SC) to improve the experimental design with reduction of the experimental work (11,49). For instance, for systems partially miscible up to a proper relevant drug dose (*e.g.*, ITZ:PVP/VA 64), a small number of solvent casting experiments with solutions containing a concentration of drug around the maximum value before phase-separation is detected, could be sufficient to provide useful information on experimental miscibility and ASD stabilization. Conversely, for systems that experience spontaneous phase-separation already at low drug loads (e.g. ITZ:Eudragit® EPO), it would probably be a poor decision to experimentally test systems with drug loads well above the minimum tested, due to the high probability of drug-polymer immiscibility. Finally, estimates such as the ones obtained for the ITZ:HPMCAS-MG system, where the model predicted total miscibility for the entire drug load range, should not be over interpreted because a formulation with 85% (w/w) drug concentration may present a higher risk of drug recrystallization, as observed for ITZ.

Based on these results, it can be verified that optimal spray dried ASDs can be produced using less time and resources, owing to the early implementation of screening methodologies that work as important decision-making elements for the rationale design of new amorphous products. Through a correct validation of the proposed methodology, it can be used not only to rank the best polymers and define a safe drug load/miscibility window, but also to study the influence of changing the solvent(s), solution composition and drying

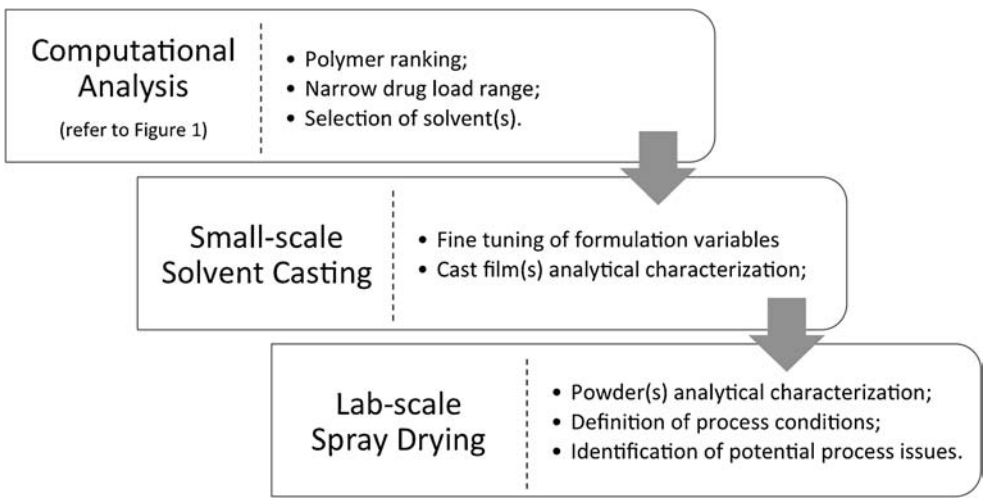

Fig. 9 Workflow for the early development of a new spray dried amorphous solid dispersion.

temperature on the final phase behavior of ASDs. A workflow demonstrating the implementation of the screening program developed in this work is shown in Fig. 9.

CONCLUSIONS

In this work, a screening methodology was developed to support the early development of spray dried amorphous solid dispersions. One of the main improvements in relation with other screening methodologies is the application of a computational tool based on diffuse interface theories for studying drug-polymer microstructure evolution.

Simulations were run for three ITZ-based systems (at increasing drug loading), with the Thermodynamic, Kinetic and Evaporation (TKE) model being able to globally describe the amorphous drug-polymer compatibility and phase behavior on the basis of the computational predictions and experimental results obtained through solvent casting and spray drying. The polymer ranking by ascending order of physical stability as determined by the model - Eudragit® EPO<< PVP/VA 64<HPMCAS-MG – was consistent with the experimental data. The miscibility of ITZ in PVP/VA 64 was higher than HPMCAS-MG, or Eudragit® EPO. Despite differences observed in the absolute maximum miscibility values obtained, it is still possible to use the information given by the TKE model to create guidelines to define a narrow drug load range to be tested in the following stages of process development, thus saving time and resources.

ACKNOWLEDGMENTS AND DISCLOSURES

Íris Duarte would like to thank the financial support from Hovione Farmaciência SA and from Fundação para a Ciência e Tecnologia through the doctoral grant BDE/51422/2011.

REFERENCES

1. Lipp R. The Innovator Pipeline: Bioavailability Challenges and Advanced Oral Drug Delivery Opportunities. American Pharmaceutical Review. 2013;16(3).
2. Thayer AM. Finding Solutions: Custom Manufacturers Take On Drug Solubility Issues To Help Pharmaceutical Firms Move Products Through Development. Chem Eng News. 2010;88(22):13–8.
3. Perrie Y, Rades T. Pharmaceutics - Drug Delivery and Targeting: Pharmaceutical Press; 2010.
4. Smithey D, Gao P, Taylor L. Amorphous solid dispersions: An enabling formulation technology for oral delivery of poorly water soluble drugs. AAPS Newsmagazine. 2013;16(1):11–4.
5. Newman A, Knipp G, Zografi G. Assessing the Performance of Amorphous Solid Dispersions. J Pharm Sci. 2012;101:1355–77.
6. [Online]. Accessed December 2013. Available from: http://www.pharma-iq.com/preclinical-discovery-and-development/articles/ensuring-stability-the-biggestamorphous-challenge/.
7. Janssens S, Van den Mooter G. Review: physical chemistry of solid dispersions. J Pharm Pharmacol. 2009;61:1571–86.
8. Van den Mooter G. The use of amorphous solid dispersions: A formulation strategy to overcome poor solubility and dissolution rate. Drug Discovery Today: Technologies. 2012;9(2):e79–85.
9. Marsac P, Shamblin S, Taylor LS. Theoretical and practical approaches for prediction of drug-polymer miscibility and solubility. Pharm Res. 2006;23(10):2417–26.
10. Tian Y, Booth J, Meehan E, Jones DS, Li S, Andrews P. Construction of Drug−Polymer Thermodynamic Phase Diagrams Using Flory−Huggins Interaction Theory: Identifying the Relevance of Temperature and Drug Weight Fraction to Phase Separation within Solid Dispersions. Mol Pharm. 2013;10:236–48.
11. Tian Y, Caron V, Jones DS, Healy AM, Andrews GP. Using Flory-Huggins phase diagrams as a pre-formulation tool for the production of amorphous solid dispersions: a comparison between hot-melt extrusion and spray drying. J Pharm Pharmacol. 2014;66(2):256–74.
12. Zhao Y, Inbar P, Chokshi HP, Malick AW, Choi DS. Prediction of the thermal phase diagram of amorphous solid dispersions by Flory-Huggins theory. J Pharm Sci. 2011;100(8):3196–207.
13. Paudel A, Nies E, Van den Mooter G. Relating hydrogen-bonding interactions with the phase behavior of naproxen/PVP K 25 solid dispersions: Evaluation of solution-casted and quench-cooled films. Mol Pharm. 2012;9(11):3301–17.
14. Bellantone RA, Patel P, Sandhu H, Choi DS, Singhal D, Chokshi H, et al. A Method to Predict the Equilibrium Solubility of Drugs in Solid Polymers near Room Temperature Using Thermal Analysis. J Pharm Sci. 2012;101(12):4549–58.
15. Kyerematen SO, Pudlas M, Woehrle GH. A Fast and Reliable Empirical Approach for Estimating Solubility of Crystalline Drugs in Polymers for Hot-Melt Extrusion Formulations. Journal of Pharmaceutical Sciences. 2014.
16. Mahieu A, Willart JF, Dudognon E, Danède F, Descamps. A new protocol to determine the solubility of drugs into polymer matrixes. Mol Pharm. 2013;10(2).
17. Tao J, Sun Y, Zhang GGZ, Yu L. Solubility of Small-Molecule Crystals in Polymers: D-Mannitol in PVP, Indomethacin in PVP/VA, and Nifedipine in PVP/VA. Pharm Res. 2009;26(4).
18. Greenhalgh DJ, Willimans AC, Timmins P, York P. Solubility parameters as predictors of miscibility in solid dispersions. J Pharm Sci. 1999;88(11):1182–90.
19. Forster A, Hempenstall J, Tucker I, Rades. Selection of excipients for melt extrusion with two poorly water-soluble drugs by solubility parameter calculation and thermal analysis. Int J Pharm. 2001;226:147–61.
20. Marsac PJ, Rumondor AC, Nivens DE, Kestur US, Stanciu L, Taylor LS. Effect of Temperature and Moisture on the Miscibility of Amorphous Dispersions of Felodipine and Poly(vinyl pyrrolidone). J Pharm Sci. 2010;99(1):169–85.
21. Albers J, Matthée K, Knop K, Kleinebudde P. Evaluation of predictive models for stable solid solution formation. 2011;100(2):667–80.
22. Keen JM, Martin, Machado A, Sandhu, McGinity JW, DiNunzio JC. Investigation of process temperature and screw speed on properties of a pharmaceutical solid dispersion using corotating and counter-rotating twin-screw extruders. J Pharm Pharmacol. 2014;66(2):204–17.
23. Saylor DM, Kim CS, Patwardhan DV, Warren JA. Diffuse-interface theory for structure formation and release behavior in controlled drug release systems. Acta Biomater. 2007;3:851–64.
24. Saylor DM. Predicting Microstructure Evolution in Controlled Drug Release Coatings. In FDA/NHLBI/NSF Workshop on Computer Methods for Cardiovascular Devices ; 2010; USA.
25. Guyer JE, Wheeler D, Warren JA. FiPy:Partial Differential Equations with Python. Computing in Science & Engineering. 2009;11(3):6–15.
26. Krevlen DW. Nijenhuis Kt. Properties of Polymers Amsterdam: Elsevier; 2009.

27. Lin D, Huang Y. A thermal analysis method to predict the complete phase diagram of drug-polymer solid dispersions. Int J Pharm. 2010;399(1–2):109–15.
28. Kawakami K, Hasegawa Y, Deguchi K, Ohki S, Shimizu T, Yoshihashi Y, et al. Competition of Thermodynamic and Dynamic Factors During Formation of Multicomponent Particles via Spray Drying. J Pharm Sci. 2013;102(2):518–29.
29. Wilke CR, Chang P. Correlation of diffusion coeficients in dilute solutions. AIChE Journal. 1955;: p. 264-270.
30. Masters K. Spray Drying in Practice Denmark: SprayDry Consult. 2002.
31. Goula AM, Adamopoulos KG. Influence of Spray Drying Conditions on Residue Accumulation - Simulation Using CFD. Dry Technol. 2004;22(5):1107–28.
32. Poling BE, Prausnitz JM. O'Connell JP. The Properties of Gases and Liquids: McGraw-Hill; 2001.
33. Miller RS, Harstad K, Bellan J. Evaluation of equilibrium and non-equilibrium evaporation models for many-droplet gas-liquid flow simulations. Int J Multiphase Flow. 1998;24:1025–55.
34. Paudel A, Humbeeck JV, Van den Mooter G. Theoretical and Experimental Investigation on the Solid Solubility and Miscibility of Naproxen in Poly(vinylpyrrolidone). Mol Pharm. 2010;7(4):1133–48.
35. Baird JA, Taylor LS. Evaluation of amorphous solid dispersion properties using thermal analysis techniques. Adv Drug Deliv Rev. 2012;64(5):396–421.
36. Six K, Verreck G, Peeters, Binnemans, Berghmans, Augustijns, et al. Investigation of thermal properties of glassy itraconazole: identification of a monotropic mesophase. Thermochim Acta. 2001;376:175–81.
37. Fedors RF. A Method for Estimating Both the Solubility Parameters and Molar Volumes of liquids. Polym Eng Sci. 1974;14(2):147–54.
38. Barton AFM. Handbook of Solubility Parameters and Other Cohesion Parameters Florida: Boca Raton, CRC Press; 1983
39. Janssens S, de Armas N, Autry D, Van S, den Mooter V. Characterization of ternary solid dispersions of Itraconazole in polyethylene glycol 6000/polyvidone-vinylacetate 64 blends. Eur J Pharm Biopharm. 2008;69:1114–20.
40. Marsac PJ, Li T, Taylor LS. Estimation of drug polymer miscibility and solubility in amorphous solid dispersions using experimentally determined interaction parameters. Pharm Res. 2009;26(1):139–51.
41. Six K, Verreck G, Peeters J, Brewster M, Van den Mooter G. Increased Physical Stability and Improved Dissolution Properties of Itraconazole, a Class II Drug, by Solid Dispersions that Combine Fast- and Slow-Dissolving Polymers. J Pharm Sci. 2004;93(1):124–31.
42. Marsac PJ, Li T, Taylor LS. Estimation of drugpolymer miscibility and solubility in amorphous solid dispersions using experimentally determined interaction parameters. Pharm Res. 2009;26(1):139–51.
43. Overhoff, Moreno A, Miller DA, Johnston P, Williams III RO. Solid dispersions of itraconazole and enteric polymers made by ultra-rapid freezing. Int J Pharm. 2007;336:122–32.
44. Rumondor CF, Wikström H, Eerdenbrugh V, Taylor LS. Understanding the Tendency of Amorphous Solid Dispersions to Undergo Amorphous–Amorphous Phase Separation in the Presence of Absorbed Moisture. AAPS PharmSciTech. 2011;12(4):1209–19.
45. Janssens S, Nagels S, de Novoa HA, Van Schepdael A, Van den Mooter G. Formulation and characterization of ternary solid dispersions made up of Itraconazole and two excipients, TPGS 1000 and PVPVA 64, that were selected based on a supersaturation screening study. Eur J Pharm Biopharm. 2008;69:158–66.
46. Vasanthavada M, Tong WQ, Joshi, Kislalioglu. Phase Behavior of Amorphous Molecular Dispersions I: Determination of the Degree and Mechanism of Solid Solubility. Pharm Res. 2004;21(9):1598–606.
47. van Drooge DJ, Hinrichs WLJ, Visser MR, Frijlink HW. Characterization of the molecular distribution of drugs in glassy solid dispersions at the nano-meter scale, using differential scanning calorimetry and gravimetric water vapour sorption techniques. Int J Pharm. 2006;310:220–9.
48. Pharmaceutical Development. ICHQ8(R2). Geneva: International Conference on Harmonisation; 2009.
49. Janssens S, Zeure AD, Paudel A, Humbeeck JV, Rombaut P, Van den Mooter G. Influence of Preparation Methods on Solid State Supersaturation of Amorphous Solid Dispersions: A Case Study with Itraconazole and Eudragit E100. Pharm Res. 2010;27(5):775–85.